A Computational Analysis of the Reaction of Atomic Oxygen O(^{3}P) with Acrylonitrile

Luca Mancini[1(✉)] and Emília Valença Ferreira de Aragão[1,2]

[1] Dipartimento di Chimica, Biologia e Biotecnologie, Università degli Studi di Perugia, 06123 Perugia, Italy
{luca.mancini2,emilia.dearagao}@studenti.unipg.it
[2] Master-Tec SrL, Via Sicilia 41, 06128 Perugia, Italy
emilia.dearagao@master-tec.it

Abstract. The work is focused on the characterization of a long-range interacting complex in the reaction between atomic oxygen, in its ground state O(^{3}P) and acrylonitrile CH_2CHCN, also known as vinyl cyanide or cyano ethylene, through electronic structure calculations. Different ab initio methods have been used in order to understand which functional provides a better description of the long-range interaction. The results of the work suggest that B2PLYPD3 gives the best description of the long-range interaction, while CAM-B3LYP represents the best compromise between chemical accuracy and computational cost.

Keywords: Ab initio calculations · Astrochemistry · Combustion chemistry

1 Introduction

The reaction between atomic oxygen, in its ground electronic state O(^{3}P) and acrylonitrile can be of great interest in several fields, such as astrochemistry and combustion chemistry.

The study of planets and moons which share similarities with primitive Earth is fundamental to understand the evolution of the prebiotic chemistry in our planet, since the appearance of life has drastically changed the characteristics of Earth. One of the best candidates for this purpose is Titan, Saturn's largest moon as well as one of the few moons of the Solar System, which possess a thick atmosphere.

The presence of acrylonitrile in Titan's atmosphere has been inferred by the detection of ionic species using Cassini mass spectrometer [1,2] and later confirmed in 2017 by the first spectroscopic detection of the molecule by ALMA (Atacama Large Millimeter/submillimeter Array) [3]. The reaction with atomic oxygen can be a destruction route of acrylonitrile, even though oxygenated species in the atmosphere of Titan are not abundant [4–6]. This process can be at play also in the Interstellar Medium, also known with the acronym ISM.

© Springer Nature Switzerland AG 2021
O. Gervasi et al. (Eds.): ICCSA 2021, LNCS 12958, pp. 339–350, 2021.
https://doi.org/10.1007/978-3-030-87016-4_25

The first detection of acrylonitrile goes back to 1975 towards the SgrB2 molecular cloud [7]. This represents the first detected molecule containing a carbon-carbon double bond. Since the first detection, the presence of acrylonitrile has been revealed in a wide variety of environments, such as the TMC-1 dark cloud where, in 1983, four rotational transitions at 3 cm and 1.5 cm were observed for the first time [8]. An analysis of the excitation of several rotational transitions has been performed, in 1999, towards the SgrB2(N) hot molecular core [9], while later in 2008 the CH_2CHCN molecule has been detected in the C-rich star IRC +10216 [10]. The analysis of the relatively high rotational temperature brought the authors to the conclusion that this species is excited in the circumstellar envelope by radiative pumping to excited vibrational states. Later in 2014 A. Lopez-Sepulcre et al. reported a new laboratory characterization in the 19–1983 GHz range, together with new astronomical detection between 80 and 280 GHz of acrylonitrile in its ground and vibrationally excited states with the IRAM-30m facilities [11]. A new analysis of the L1154 prestellar core has been carried out in 2019, where several N-containing species have been detected for the first time [12]. The inventory of the aforementioned molecules includes small and simple species such ah CN and NCCN, together with more complex species like CH_3CN, CH_2CN, HCCNC and CH_2CHCN. A detailed chemical network has been built involving all the nitrogen bearing species detected in order to understand the isocyanogen formation in the ISM. Moreover, the reactions of $O(^3P)$ with these substrates play a key role in combustion science and atmospheric chemistry [13–18], considering the ease with which this species is formed and the high reactivity. The presence of nitrogen atoms in several fuels or biomass combustion [19] makes it interesting to investigate the reaction of oxygen atoms with these substrates.

In the present work we performed a theoretical study of the first step of the reaction of acrylonitrile with atomic oxygen, focusing our interest on the analysis of different theoretical methods which can be used for the identification of a van der Waals adduct in the entrance channel.

The presence of a van der Waals adduct can affect the chemical reactivity of bimolecular reactions as it was already found in several systems [20–24].

The title reaction has been already investigated theoretically by J. Sun et al. [25] who performed an exploration of the triplet potential energy surface. An experimental characterization has been performed by H. P. Upadhyay et al. [26] in a flow discharge tube using the $O(^3P)$ chemiluminescence titration method. More generally it is reasonable to think that the formation of a van der Waals adduct is one of the first stages of most of the reactions. The long-range interaction in the formed complex can lead to molecular geometries that can promote or hinder the evolution of the reaction. As a consequence the formation of a van der Waals complex can strongly affect the rate constants. Unfortunately the identification of the aforementioned complexes appears to be difficult with mostly used ab initio methods. In the following sections a comparison between the results obtained at different levels of theory is presented. In particular the analysis started with a benchmark work in order to compare different methods,

see next sections for more details, while the last part of the work is focused on the comparison between two particular level of theory: B3LYP and CAM-B3LYP.

2 Methods

The investigation of the title system has been performed adopting a computational strategy which has been successfully used in several cases [27–36]. In particular electronic structure calculations have been performed for the reactants and for the long-range complex on the overall triplet Potential Energy Surface (PES). In all calculations, the geometries of the stationary points were treated with two different methods: one for optimization and another to obtain more accurate energy values. Geometry optimizations were performed in order to benchmark several methods: density functional theory (DFT), with the BHandHLYP functional [37,38]; the Becke-3-parameter exchange and Lee-Yang- Parr correlation (B3LYP) [39,40] combined or not with Grimme's D3BJ [41,42] dispersion (B3LYPD3); Coulomb Attenuating Method (CAM-B3LYP) [43]; double-hybrid DFT method B2PLYP [44] combined or not with Grimme's D3BJ dispersion (B2PLYPD3) and the long-range corrected functional ωB97X [45] also with the inclusion of both Grimme's D2 and D3 dispersion model (ωB97XD; ωB97XD3) [46–48]. In particular the aforementioned functional, named CAM-B3LYP (Coulomb Attenuating Method-B3LYP) represents a new hybrid exchange-correlation functional with improved long-range properties with respect to the B3LYP [43]. In detail, the electron repulsion operator $\frac{1}{r_{12}}$, which was already divided into short-range and long-range parts by Tsuneda and collaborators [49] as follows:

$$\frac{1}{r_{12}} = \frac{1 - erf(\mu r_{12})}{r_{12}} + \frac{erf(\mu r_{12})}{r_{12}} \tag{1}$$

is now implemented using two parameters α and β:

$$\frac{1}{r_{12}} = \frac{1 - [\alpha + \beta * erf(\mu r_{12})]}{r_{12}} + \frac{\alpha + \beta * erf(\mu r_{12})}{r_{12}} \tag{2}$$

where $0 \leq \alpha + \beta \leq 1$ together with $0 \leq \alpha \leq 1$ and $0 \leq \beta \leq 1$.

All the above mentioned methods have been used in conjunction with the correlation consistent valence polarized basis set aug-cc-pVTZ [50]. The same level of theory used for geometry optimization was used to perform a vibrational frequency analysis in order to assign the nature of each identified stationary point (i.e. minimum if all the frequencies are real and saddle point if there is one, and only one, imaginary frequency). Then for each stationary point for all the employed methods, a more accurate energy value was computed at coupled cluster level, including single and double excitations as well as perturbative estimate of connected triples (CCSD(T)) [51–53]. Finally, energies obtained from every method were corrected to 0 K by adding the zero-point energy correction derived from the frequency calculations.

All the calculations were performed using the Gaussian09 software [54], while the analysis of the vibrational frequencies was done using Avogadro [55].

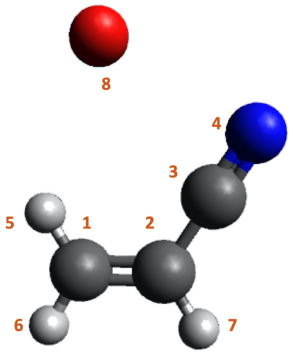

Fig. 1. Geometry of the long-range identified complex

Table 1. Bond distances, in Å, obtained at the different level of theory

Dist./ Funct	B3LYP	B3LYP-D3	CAM-B3LYP	B2PLYP	B2PLYP-D3	ωB97X	ωB97XD	ωB97XD3	BHandHLYP
C_1-H_5	1.081	1.081	1.080	1.079	1.079	1.082	1.081	1.082	1.073
C_1-H_6	1.080	1.081	1.080	1.079	1.079	1.081	1.081	1.081	1.073
C_1-C_2	1.331	1.331	1.324	1.334	1.334	1.325	1.327	1.326	1.320
C_2-H_7	1.083	1.083	1.081	1.081	1.081	1.082	1.082	1.082	1.074
C_2-C_3	1.426	1.426	1.428	1.428	1.428	1.435	1.430	1.435	1.425
C_3-N_4	1.154	1.154	1.146	1.161	1.161	1.149	1.149	1.149	1.139
O_8-C_1	3.643	3.444	3.584	3.634	3.573	3.462	3.601	3.399	3.633
O_8-C_2	3.758	3.590	3.735	3.830	3.764	3.615	3.834	3.566	3.860
O_8-C_3	2.996	2.883	3.001	3.131	3.069	2.893	3.171	2.867	3.193
O_8-N_4	2.794	2.787	2.848	2.995	2.954	2.771	3.066	2.775	3.077
O_8-H_5	2.853	2.647	2.773	2.793	2.738	2.655	2.740	2.588	2.778

3 Results and Discussion

The data obtained from electronic structure calculations clearly show the formation of a long-range complex as the first step of the reaction between O(^{3}P) and acrylonitrile. The process appears to be exothermic at all the previously cited levels of theory. The structure of the complex shows the interaction of the oxygen atom with the double bond between C_1 and C_2 of the CH_2CHCN molecule. In Table 1 are reported the bond distances, expressed in angstroms, obtained at the different levels of theory. The geometry of the complex with all the atom labels is reported in Fig. 1. A comparison between the values of bond distances obtained with the different theoretical methods can bring to the conclusion that there are no significant differences in the values of the distances related to covalent bonds,

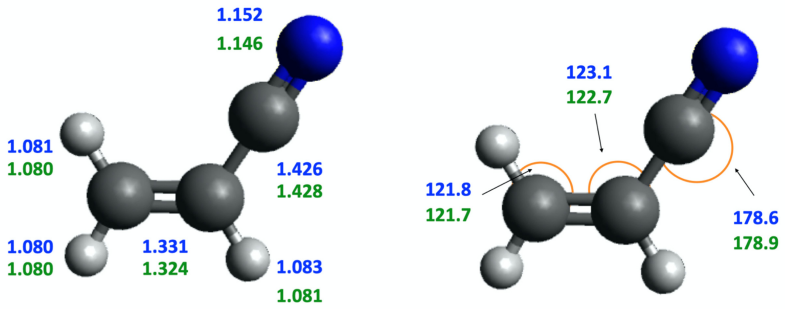

Fig. 2. Bond lengths (Å) and angles for the reactant at the B3LYP/aug-cc-pVTZ (blue) and CAM- B3LYP/aug-cc-pVTZ (green) level of theory. (Color figure online)

Table 2. Energies obtained at the different level of theory, with respect to the reactant energy asymptote.

Method	$E_{REL(Method)}$	$E_{REL(CCSD(T))}$
	kJ mol^{-1}	kJ mol^{-1}
B3LYP	-3.0	-5.1
B3LYP-D3	-8.0	-4.3
CAM-B3LYP	-4.3	-5.3
B2PLYP	-0.9	-5.7
B2PLYP-D3	-2.4	-5.5
ωB97X	-7.6	-4.1
ωB97XD	-4.0	-5.7
ωB97XD3	-11.1	-3.8
BHandHLYP	-3.0	-5.9

such as C-C, C-H and C-N, how can be seen also from the comparison of the structure of the reactant in Fig. 2. Nevertheless some discrepancies can be noted in the description of the long-range interaction. In particular it is possible to notice some differences in the interaction distance O_8-C_5 between B3LYP and CAM-B3LYP functionals. As expected, the use of CAM-B3LYP with respect to B3LYP allows us to obtain results more in line with other functionals which include the dispersion effects, such as B2PLYPD3 and ωB97XD3. In order to have a better comprehension of the differences between the methods it is possible to compare the energies obtained from the various calculations.

In Table 2 the energies obtained at the different levels of theory are reported. In particular the first column reports the electronic energies computed at the defined level of theory (in kJ mol^{-1}), while in the last column are reported the values obtained by the CCSD(T) calculations starting from the geometry optimized at the lower level of theory. The values are corrected at 0 K including the zero point correction obtained from the harmonic vibrational calculations

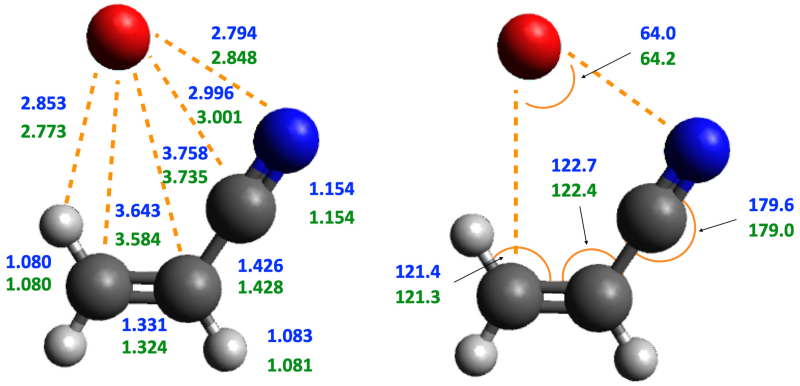

Fig. 3. Bond lengths (Å) and angles for the vdW adduct at the B3LYP/aug-cc-pVTZ (blue) and CAM-B3LYP/aug-cc-pVTZ (green) level of theory. (Color figure online)

performed at the same level of theory used for the geometry optimization. The analysis of the values of energy reported in Table 2 shows no significant differences in the values of the CCSD(T) corrected energy, which is usually considered in the construction of the potential energy surface. In particular we can notice that most of the time the difference is lower than 5 kJ mol^{-1}, which is considered to be the uncertainty associated to accurate calculations.

Since no significant differences can be noticed between the employed methods we decided to focus our attention on the comparison between the B3LYP method and CAM-B3LYP, which is presented as an improvement of the B3LYP in order to include the long-range interaction. In Figs. 2 and 3 a comparison of the bond distances (in Å) and angles (in °) between the two methods is reported for the reactant (vinyl cyanide) and for the complex respectively. The results of the B3LYP/aug-cc-pVTZ analysis are shown in blue while the values derived from the CAM-B3LYP/aug-cc-pVTZ calculations are displayed in green.

As previously mentioned the main differences can be appreciated in the description of the long-range O-C interaction with deviations lower than 0.1 Å for the bond distances and of a maximum of 0.6° for the angles. The analysis of the harmonic vibrational frequencies, reported in Table 3, shows small differences between the two levels of theory. In particular it can be important to compare the first two rows (named a and b) related to the O_8-H_5 and O_8-N_4 intermolecular stretching. The c-m values reported in Table 3 are related to the intramolecular bonding, while the n-r values are related to the intramolecular stretching. These differences lead to a small variation on the zero-point correction which is equal to 134.1 kJ mol^{-1} at B3LYP/aug-cc-pVTZ and 135.7 kJ mol^{-1} at CAM-B3LYP/aug-cc-pVTZ level of theory.

Table 3. Harmonic vibrational frequencies (cm^{-1}) of the vdW adduct obtained at the B3LYP/aug-cc-pVTZ and CAM-B3LYP/aug-cc-pVTZ level of theory.

	B3LYP	CAM-B3LYP
a	54.1	62.9
b	75.3	74.8
c	43.6	42.3
d	237.2	242.4
e	354.5	360.2
f	585.9	592.6
g	713.1	725.3
h	882.7	890.3
i	1005.3	1019.4
j	1008.8	1033.0
k	1113.1	1122.4
l	1324.1	1333.9
m	1448.5	1456.9
n	1672.3	1712.2
o	2319.8	2386.6
p	3155.7	3175.6
q	3171.6	3202.0
R	3248.8	3269.4

A last comparison between the two methods, together with the B2PLYPD3 method, can be performed considering the first steps of the reaction, shown in Fig. 4. The reaction starts with a barrierless formation of the previously described complex, MIN1, followed by the formation of the minimum MIN2 in which we can notice the formation of a chemical bond between C_1 and O, through a small barrier, represented by TS1. No particular differences can be noticed in the values of energy obtained at CCSD(T)/aug-cc-pVTZ level considering the geometries optimized at B3LYP level (in blue) and at CAM-B3LYP (in green) level of theory. A last comparison can be done between two other methods, such as CAM-B3LYP and B2PLYPD3. As can be seen in Fig. 4, some small discrepancies are present between the two methods. Nevertheless all the aforementioned differences are smaller then the uncertainty of accurate calculations.

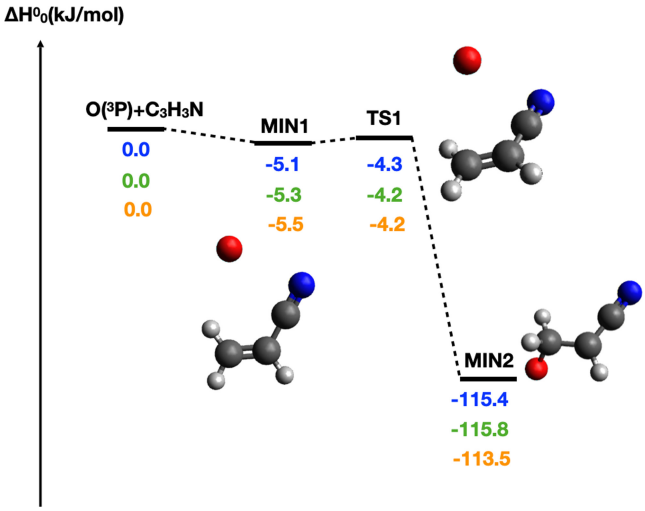

Fig. 4. Schematic representation of the potential energy surface for the first steps of the attack of the O(^{3}P) atom to the acrylonitrile molecule. Energies are computed at CCSD(T)/aug-cc-pVTZ level with zero-point corrections at B3LYP/aug-cc-pVTZ (blue), CAM-B3LYP/aug-cc-pVTZ (green) and B2PLYPD3/aug-cc-pVTZ (orange) levels of theory. (Color figure online)

4 Conclusions

In the present work we performed a benchmark analysis of the first step of the reaction between atomic oxygen O(^{3}P) and acrylonitrile (CH_2CHCN) using different theoretical methods: DFT (with BHandHLYP, B3LYP and B3LYPD3 functional), double-hybrid DFT (with B2PLYP and B2PLYPD3 functionals) and the long-range corrected functional ωB97X, ωB97XD and ωB97XD3. As far as optimized geometries for stationary points are concerned, all the methods seem to provide similar results. In particular, the B3LYP functional appears to be a good compromise between accuracy and computational cost for the characterization of minima. The analysis of the long-range interaction can be performed also using the CAM-B3LYP functional, which provides better estimate of the interactions than the B3LYP functional but needs lower computational resources than the B2PLYPD3 functional. The best choice for the estimate of the energies appears to be the use of correlated methods like CCSD(T). A more general conclusion can be presented concerning the first steps of the reaction mechanism, which appears to be in agreement with the previous determination by J. Sun et al. [25]. In particular the oxygen atom starts to interact with the electron density of multiple bonds in the molecule to form an exothermic addition intermediate. The comparison with B3LYP and CAM-B3LYP functionals suggests the possibility to use a combined strategy for the analysis of the Potential Energy Surfaces which will allow us to locate the long-range complexes at CAM-B3LYP level to be included in the reaction pathways.

Acknowledgements. This project has received funding from the European Union's Horizon 2020 research and innovation programme under the Marie Skłodowska-Curie grant agreement No 811312 for the project "Astro-Chemical Origins" (ACO). This work was supported by the Italian Space Agency (ASI) BANDO ASI DC-VUM-2017-034 CONTRATTO DI FINANZIAMENTO ASI N. 2019-3 U.O, "Vita nello spazio - Origine, presenza, persistenza della vita nello spazio, dalle molecole agli estremofili". The authors acknowledge the Dipartimento di Ingegneria Civile e Ambientale of the University of Perugia for allocated computing time within the project "Dipartimenti di Eccellenza 2018–2022".

References

1. Vuitton, V., Yelle, R., McEwan, M.: Ion chemistry and n-containing molecules in Titan's upper atmosphere. Icarus **191**(2), 722–742 (2007)
2. Cui, J., et al.: Analysis of Titan's neutral upper atmosphere from Cassini ion neutral mass spectrometer measurements. Icarus **200**(2), 581–615 (2009)
3. Palmer, M.Y., et al.: Alma detection and astrobiological potential of vinyl cyanide on Titan. Sci. Adv. **3**(7), e1700022 (2017)
4. Feuchtgruber, H., et al.: Oxygen in the stratospheres of the giant planets and Titan. In: The Universe as Seen by ISO, vol. 427, p. 133 (1999)
5. Teanby, N., et al.: The origin of Titan's external oxygen: further constraints from ALMA upper limits on CS and CH2NH. Astron. J. **155**(6), 251 (2018)
6. Hörst, S.M., Vuitton, V., Yelle, R.V.: Origin of oxygen species in Titan's atmosphere. J. Geophys. Res. Planets **113**(E10), 1–14 (2008)
7. Gardner, F., Winnewisser, G.: The detection of interstellar vinyl cyanide/acrylonitrile. Astrophys. J. **195**, L127–L130 (1975)
8. Matthews, H.E., Sears, T.J.: The detection of vinyl cyanide in TMC-1. Astrophys. J. **272**, 149–153 (1983)
9. Nummelin, A., Bergman, P.: Vibrationally excited vinyl cyanide in SGR B2(N). Astron. Astrophys. **341**, L59–L62 (1999)
10. Agúndez, M., Fonfría, J.P., Cernicharo, J., Pardo, J., Guélin, M.: Detection of circumstellar CH2CHCN, CH2CN, CH3CCH, and H2CS. Astron. Astrophys. **479**(2), 493–501 (2008)
11. López, A., et al.: Laboratory characterization and astrophysical detection of vibrationally excited states of vinyl cyanide in Orion-KL. Astron. Astrophys. **572**, A44 (2014)
12. Vastel, C., Loison, J.C., Wakelam, V., Lefloch, B.: Isocyanogen formation in the cold interstellar medium. Astron. Astrophys. **625**, A91 (2019)
13. Cavallotti, C., et al.: Relevance of the channel leading to formaldehyde + triplet ethylidene in the O(^{3}P)+ propene reaction under combustion conditions. J. Phys. Chem. Lett. **5**(23), 4213–4218 (2014)
14. Balucani, N., Leonori, F., Casavecchia, P.: Crossed molecular beam studies of bimolecular reactions of relevance in combustion. Energy **43**(1), 47–54 (2012)
15. Cavallotti, C., et al.: Theoretical study of the extent of intersystem crossing in the O(^{3}P) + C6H6 reaction with experimental validation. J. Phys. Chem. Lett. **11**(22), 9621–9628 (2020)
16. Leonori, F., Occhiogrosso, A., Balucani, N., Bucci, A., Petrucci, R., Casavecchia, P.: Crossed molecular beam dynamics studies of the O(^{3}P) + allene reaction: primary products, branching ratios, and dominant role of intersystem crossing. J. Phys. Chem. Lett. **3**(1), 75–80 (2012)

17. Balucani, N., Leonori, F., Casavecchia, P., Fu, B., Bowman, J.M.: Crossed molecular beams and quasiclassical trajectory surface hopping studies of the multichannel nonadiabatic O(^{3}P) + ethylene reaction at high collision energy. J. Phys. Chem. A **119**(50), 12498–12511 (2015)
18. Fu, B., et al.: Experimental and theoretical studies of the O(^{3}P) + C2H4 reaction dynamics: collision energy dependence of branching ratios and extent of intersystem crossing. J. Chem. Phys. **137**(22), 22A532 (2012)
19. Simoneit, B.R., Rushdi, A., Bin Abas, M., Didyk, B.: Alkyl amides and nitriles as novel tracers for biomass burning. Environ. Sci. Technol. **37**(1), 16–21 (2003)
20. Skouteris, D., Manolopoulos, D.E., Bian, W., Werner, H.J., Lai, L.H., Liu, K.: van der Waals interactions in the CL + HD reaction. Science **286**(5445), 1713–1716 (1999)
21. Balucani, N., et al.: The dynamics of the prototype abstraction reaction Cl(^{2}P3/2,1/2) + H2: a comparison of crossed molecular beam experiments with exact quantum scattering calculations on coupled ab initio potential energy surfaces. Phys. Chem. Chem. Phys. **6**(21), 5007–5017 (2004)
22. Skouteris, D., et al.: Experimental and theoretical differential cross sections for the reactions Cl+H2/D2. J. Chem. Phys. **114**(24), 10662–10672 (2001)
23. Heard, D.E.: Rapid acceleration of hydrogen atom abstraction reactions of OH at very low temperatures through weakly bound complexes and tunneling. Acc. Chem. Res. **51**(11), 2620–2627 (2018)
24. Recio, P., et al.: Efficient intersystem crossing from weakly bound pre-reactive complex avoids the entrance barrier of bimolecular reactions. Nat. Chem. (submitted)
25. Sun, J., et al.: Theoretical investigation on atmospheric reaction of atomic O(^{3}P) with acrylonitrile. Comput. Theor. Chem. **1052**, 17–25 (2015)
26. Upadhyaya, H.P., et al.: Reaction kinetics of O(^{3}P) with acrylonitrile and crotononitrile. Chem. Phys. Lett. **274**(4), 383–389 (1997)
27. Falcinelli, S., Rosi, M., Cavalli, S., Pirani, F., Vecchiocattivi, F.: Stereoselectivity in autoionization reactions of hydrogenated molecules by metastable noble gas atoms: the role of electronic couplings. Chem. Eur. J. **22**(35), 12518–12526 (2016)
28. Leonori, F., et al.: Crossed-beam and theoretical studies of the S(^{1}D) + C_2H_2 reaction. J. Phys. Chem. A **113**(16), 4330–4339 (2009)
29. Bartolomei, M., et al.: The intermolecular potential in NO-N_2 and (NO-N_2)$^+$ systems: implications for the neutralization of ionic molecular aggregates. Phys. Chem. Chem. Phys. **10**(39), 5993–6001 (2008)
30. de Petris, G., Cartoni, A., Rosi, M., Barone, V., Puzzarini, C., Troiani, A.: The proton affinity and gas-phase basicity of sulfur dioxide. ChemPhysChem **12**(1), 112–115 (2011)
31. Leonori, F., et al.: Observation of organosulfur products (thiovinoxy, thioketene and thioformyl) in crossed-beam experiments and low temperature rate coefficients for the reaction S(^{1}D) + C_2H_4. Phys. Chem. Chem. Phys. **11**(23), 4701–4706 (2009)
32. de Petris, G., Rosi, M., Troiani, A.: SSOH and HSSO radicals: an experimental and theoretical study of $[S_2OH]^{0/+/-}$ species. J. Phys. Chem. A **111**(28), 6526–6533 (2007)
33. Rosi, M., Falcinelli, S., Balucani, N., Casavecchia, P., Leonori, F., Skouteris, D.: Theoretical study of reactions relevant for atmospheric models of Titan: interaction of excited nitrogen atoms with small hydrocarbons. In: Murgante, B., et al. (eds.) ICCSA 2012. LNCS, vol. 7333, pp. 331–344. Springer, Heidelberg (2012). https://doi.org/10.1007/978-3-642-31125-3_26

34. Berteloite, C., et al.: Low temperature kinetics, crossed beam dynamics and theoretical studies of the reaction $S(^1D) + CH_4$ and low temperature kinetics of $S(^1D) + C_2H_2$. Phys. Chem. Chem. Phys. **13**(18), 8485–8501 (2011)
35. Rosi, M., Falcinelli, S., Balucani, N., Casavecchia, P., Skouteris, D.: A theoretical study of formation routes and dimerization of methanimine and implications for the aerosols formation in the upper atmosphere of Titan. In: Murgante, B., et al. (eds.) ICCSA 2013. LNCS, vol. 7971, pp. 47–56. Springer, Heidelberg (2013). https://doi.org/10.1007/978-3-642-39637-3_4
36. Sleiman, C., El Dib, G., Rosi, M., Skouteris, D., Balucani, N., Canosa, A.: Low temperature kinetics and theoretical studies of the reaction $CN + CH_3NH_2$: a potential source of cyanamide and methyl cyanamide in the interstellar medium. Phys. Chem. Chem. Phys. **20**(8), 5478–5489 (2018)
37. Becke, A.D.: A new mixing of Hartree-Fock and local density-functional theories. J. Chem. Phys. **98**(2), 1372–1377 (1993)
38. Lee, C., Yang, W., Parr, R.G.: Development of the Colle-Salvetti correlation-energy formula into a functional of the electron density. Phys. Rev. B **37**(2), 785 (1988)
39. Becke, A.D.: Density functional thermochemistry. III. The role of exact exchange. J. Chem. Phys. **98**(7), 5648–5652 (1993). https://doi.org/10.1063/1.464913
40. Stephens, P.J., Devlin, F.J., Chabalowski, C.F., Frisch, M.J.: *Ab initio* calculation of vibrational absorption and circular dichroism spectra using density functional force fields. J. Phys. Chem. **98**(45), 11623–11627 (1994)
41. Grimme, S., Ehrlich, S., Goerigk, L.: Effect of the damping function in dispersion corrected density functional theory. J. Comput. Chem. **32**(7), 1456–1465 (2011)
42. Goerigk, L., Grimme, S.: Efficient and accurate double-hybrid-meta-GGA density functionals-evaluation with the extended GMTKN30 database for general main group thermochemistry, kinetics, and noncovalent interactions. J. Chem. Theory Comput. **7**(2), 291–309 (2011)
43. Yanai, T., Tew, D.P., Handy, N.C.: A new hybrid exchange-correlation functional using the Coulomb-attenuating method (CAM-B3LYP). Chem. Phys. Lett. **393**(1–3), 51–57 (2004)
44. Grimme, S.: Semiempirical hybrid density functional with perturbative second-order correlation. J. Chem. Phys. **124**(3), 034108 (2006)
45. Chai, J.D., Head-Gordon, M.: Systematic optimization of long-range corrected hybrid density functionals. J. Chem. Phys. **128**(8), 084106 (2008)
46. Chai, J.D., Head-Gordon, M.: Long-range corrected hybrid density functionals with damped atom-atom dispersion corrections. Phys. Chem. Chem. Phys. **10**(44), 6615–6620 (2008)
47. Lin, Y.S., Li, G.D., Mao, S.P., Chai, J.D.: Long-range corrected hybrid density functionals with improved dispersion corrections. J. Chem. Theory Comput. **9**(1), 263–272 (2013)
48. Goerigk, L., Hansen, A., Bauer, C., Ehrlich, S., Najibi, A., Grimme, S.: A look at the density functional theory zoo with the advanced GMTKN55 database for general main group thermochemistry, kinetics and noncovalent interactions. Phys. Chem. Chem. Phys. **19**(48), 32184–32215 (2017)
49. Tawada, Y., Tsuneda, T., Yanagisawa, S., Yanai, T., Hirao, K.: A long-range-corrected time-dependent density functional theory. J. Chem. Phys. **120**(18), 8425–8433 (2004)
50. Dunning, T.H., Jr.: Gaussian basis sets for use in correlated molecular calculations. I. The atoms boron through neon and hydrogen. J. Chem. Phys. **90**(2), 1007–1023 (1989)

51. Bartlett, R.J.: Many-body perturbation theory and coupled cluster theory for electron correlation in molecules. Annu. Rev. Phys. Chem. **32**(1), 359–401 (1981)
52. Raghavachari, K., Trucks, G.W., Pople, J.A., Head-Gordon, M.: A fifth-order perturbation comparison of electron correlation theories. Chem. Phys. Lett. **157**(6), 479–483 (1989)
53. Olsen, J., Jørgensen, P., Koch, H., Balkova, A., Bartlett, R.J.: Full configuration-interaction and state of the art correlation calculations on water in a valence double-zeta basis with polarization functions. J. Chem. Phys. **104**(20), 8007–8015 (1996)
54. Frisch, M., et al.: Gaussian 09, Revision A. 02, 2009, Gaussian. Inc., Wallingford CT (2009)
55. Hanwell, M.D., Curtis, D.E., Lonie, D.C., Vandermeersch, T., Zurek, E., Hutchison, G.R.: Avogadro: an advanced semantic chemical editor, visualization, and analysis platform. J. Cheminform. **4**(1), 1–17 (2012)